



OPEN ACCESS

EDITED BY

Sherin Bakhashab,
King Abdulaziz University, Saudi Arabia

REVIEWED BY

Venkata Sk Manem,
Centre de Recherche du CHU
de Québec, Canada
Vanessa Sotomaior,
Pontifícia Universidade
Católica do Paraná, Brazil

*CORRESPONDENCE

Arvind Mer

✉ amer@uottawa.ca

Benjamin K. Tsang

✉ btsang@ohri.ca

RECEIVED 11 December 2024

ACCEPTED 24 June 2025

PUBLISHED 14 July 2025

CITATION

Asare-Werehene M, Zaker A, Tripathi S,
Communal L, Carmona E, Mes-Masson A-M,
Tsang BK and Mer A (2025) Spotlight on
nuclear PD-L1 in ovarian cancer
chemoresistance: hidden but mighty.
Front. Immunol. 16:1543529.
doi: 10.3389/fimmu.2025.1543529

COPYRIGHT

© 2025 Asare-Werehene, Zaker, Tripathi,
Communal, Carmona, Mes-Masson, Tsang and
Mer. This is an open-access article distributed
under the terms of the [Creative Commons
Attribution License \(CC BY\)](#). The use,
distribution or reproduction in other forums
is permitted, provided the original author(s)
and the copyright owner(s) are credited and
that the original publication in this journal is
cited, in accordance with accepted academic
practice. No use, distribution or reproduction
is permitted which does not comply with
these terms.

Spotlight on nuclear PD-L1 in ovarian cancer chemoresistance: hidden but mighty

Meshach Asare-Werehene^{1,2,3,4}, Arvin Zaker⁵,
Shivanshi Tripathi⁵, Laudine Communal⁶, Euridice Carmona⁶,
Anne-Marie Mes-Masson⁶, Benjamin K. Tsang^{1,2,3*}
and Arvind Mer^{5,7,8*}

¹Department of Obstetrics & Gynecology, University of Ottawa, Ottawa, ON, Canada, ²Department of Cellular and Molecular Medicine & The Centre for Infection, Immunity and Inflammation (CI3), Faculty of Medicine, University of Ottawa, Ottawa, ON, Canada, ³Inflammation and Chronic Disease Program, Ottawa Hospital Research Institute, Ottawa, ON, Canada, ⁴Department of Laboratory Medicine and Pathobiology, University of Toronto, Ottawa, ON, Canada, ⁵Department of Biochemistry, Immunology and Microbiology, University of Ottawa, Ottawa, ON, Canada, ⁶Centre de recherche du CHUM et Institut du cancer de Montréal, Département de médecine, Université de Montréal, Montréal, QC, Canada, ⁷School of Electrical Engineering and Computer Science, University of Ottawa, Ottawa, ON, Canada, ⁸Ottawa Institute of Systems Biology, University of Ottawa, Ottawa, ON, Canada

Introduction: Ovarian cancer (OVCA) has a five-year survival rate of approximately 45%, with little improvement over recent decades. Although anti-PD-L1 therapies have shown substantial efficacy in other solid tumors, their effectiveness in OVCA has been limited. These treatments target only membranous and soluble forms of PD-L1, without addressing nuclear-localized PD-L1. The role of nuclear PD-L1 in OVCA chemoresistance, however, remains largely unexplored. In this study, we examined the prognostic significance of nuclear PD-L1 and its interactions with plasma gelsolin (pGSN) and CD8+ T cells within the tumor microenvironment.

Methods: Using immunofluorescence, we quantified nuclear PD-L1, pGSN, and additional markers in OVCA samples. Statistical analyses and machine learning approaches were employed to assess associations between marker expression, patient outcomes, and chemoresistance.

Results: Increased nuclear PD-L1 was associated with disease recurrence, chemoresistance and poor overall survival. Although CD8+ T cells provided survival benefits to patients, elevated PD-L1 hindered these benefits resulting in shortened disease free (DFS) and overall survival (OS). Co-expression of PD-L1 and pGSN was also associated with shortened DFS, OS and chemoresistance.

Discussion: These findings indicate that nuclear PD-L1 serves as a poor prognostic marker in OVCA, being associated with tumor recurrence, chemoresistance, and reduced overall survival. Targeting nuclear PD-L1 may represent a novel therapeutic strategy to improve outcomes in patients with OVCA.

KEYWORDS

PD-L1, immunotherapy, nuclear PD-L1, ovarian cancer, chemoresistance, tumor microenvironment, plasma gelsolin (pGSN)

Introduction

Ovarian cancer (OVCA) is a lethal gynecological malignancy with a 5-year survival rate of ~45% (1, 2). The first line treatment is surgical debulking coupled with chemotherapeutic agent. Complete cytoreductive surgery (CCR 0), where no macroscopic disease remains, is strongly associated with improved overall survival. In contrast, patients left with residual macroscopic disease (CCR 1–3) after surgery face significantly poorer outcomes. Notably, the potential for cure in cases with substantial residual tumor burden at the conclusion of surgery is exceedingly limited. These distinctions underscore the importance of optimal surgical planning and execution in improving patient prognosis. Although patients initially respond to treatment, late diagnosis and chemoresistance present as major obstacle to treatment success.

Treatment response in OVCA is modulated by the tumor microenvironment especially the immune system which plays a crucial role in the recognition and elimination of tumor cells. Interestingly, OVCA cells can evade immune surveillance by expressing immuno-suppressive molecules such as pGSN and PD-L1 (3–7). pGSN is highly expressed in OVCA tissues and activates the Akt/HIF1alpha axis resulting in chemoresistance (8). Increased expression of pGSN by OVCA tissues inhibits the anti-tumor functions of CD8+ T cells, dendritic cells, NK cells and macrophages in the tumor microenvironment leading to tumor recurrence, chemoresistance and poor survival (9–12).

PD-L1 binds to its receptor, programmed death 1 (PD1), on the surface of T cells and inhibits their activation and function, resulting in reduced T cell cytotoxicity and increased tumor growth (13–15). Previous studies have shown conflicting results regarding the prognostic value of PD-L1 in the ovarian tumor microenvironment (15). A study by Høgdall et al., revealed that PD-L1 over-expression was observed in ~50% of all OVCA cases and associated with advanced stage and tumor aggressiveness (16). Meanwhile other studies have shown a positive correlation between PD-L1 expression and T cell infiltration suggesting PD-L1 expression as a potential predictive biomarker for immunotherapy (17–19). Investigation into the underlying functional dynamics of PD-L1 is crucial for developing highly effective and personalized therapies to achieve optimal responses in ovarian cancer patients. Targeting the PD-L1/PD1 axis is a promising strategy to enhance antitumor immunity and improve clinical outcomes in many malignancies. Despite the significant treatment responses achieved in other solid cancers, anti-PD-L1 inhibitors have produced only modest therapeutic success in OVCA patients (20–23). These conventional antibodies only target membranous and soluble PD-L1 without any effect on intracellular PD-L1. Nuclear PD-L1 has recently been detected in a variety of malignancies including breast cancer, colon cancer, lung cancer and prostate cancers (23–27). Although their function in the nucleus is not well established, it's been shown to induce transcription of genes leading to angiogenesis, tumorigenesis, drug resistance and tumor recurrence (26–28). It is currently unknown if nuclear PD-L1 is detectable in OVCA tissues. Whether its presence in OVCA tissue

might explain the modest therapeutic responses seen with anti-PD-L1 immunotherapies is not known.

In this study, we report for the first time the detection and prognostic value of PD-L1 expression in the nucleus and cytoplasm of OVCA tissues. We also provide findings on the relationship between nuclear PD-L1, pGSN and T cells and how their interaction correlates with tumor recurrence, chemoresistance and patient survival.

Materials and methods

Ethics statement and tissue sampling

The study was in accordance with the appropriate guidelines approved by the Centre hospitalier de l'Université de Montreal (CHUM) Ethics Committee [Montreal, Quebec, Canada, Institutional Review Board (IRB) approval number, BD 04-002] and the Ottawa Health Science Network Research Ethics Board (Ottawa, Ontario, Canada, IRB approval number, OHSN-REB 1999540-01H). 208 subjects enrolled in the study were treatment naïve patients with OVCA from 1992–2012 at the CHUM (Montreal, Quebec, Canada) and provided written informed consent. Thus, these patients received no radiotherapy nor neoadjuvant chemotherapy prior to sample collection at surgery. Tissue microarrays (TMA) were built with a total of 208 formalin-fixed OVCA tissue samples, 14 normal fallopian tube samples and cell line pellets (TOV122D and OV2295) in duplicates. Details of patient population is described in Table 1. BRCA status was unavailable for a subset of samples, resulting in a total count lower than the full cohort (n=208) in Table 1. Patients were diagnosed, tissues examined, and clinical data gathered as described previously (9).

Immunofluorescence

BenchMark XT automated stainer (Ventana Medical System Inc. Tucson, AZ) was used for the immunostaining of the OVCA Tissue Microarray (TMA). Tissues were taken through deparaffinization, antigen retrieval and antibody staining as previously described (9). Antibody cocktail against mouse anti-cytokeratin 7, 18 (Santa Cruz Biotechnology; ref. sc-5659) and 19 (NBP2-15186; ref. 1P170302; Novus Biologicals) coupled with Cy5 anti-mouse secondary antibody (Invitrogen; ref. A21236; lot #: 2119453) were used for the keratin staining. Anti-CD8 mouse monoclonal (Leica Biosystems; NCL-L-CD8-4B11) coupled with anti-mouse TRITC secondary antibody IgG2b 594 (Invitrogen; ref. A21145) were used for the CD8 staining. Anti-PDL1 rabbit antibody (Sigma-Aldrich; Ref. PRS4059) coupled with anti-rabbit AF488 secondary antibody (Invitrogen, ref. A11008; lot #: 2284594) were used for the PDL1 staining. In a separate panel, anti-pGSN mouse polyclonal (Antibodies online, ref. ABIN659182) coupled with anti-mouse AF647 (Invitrogen, ref. A21240; lot #: 2185066) were used for the pGSN staining. Dapi was used to stain the nuclei of the cells after which the

TABLE 1 Clinical characteristics of the patients used in the analysis.

Variables	All	BRCA non-carriers	BRCA1 carriers	BRCA2 carriers	P
N	208	127	14	17	
Age (mean ± SD)	61.75 ± 10.26	63.14 ± 9.09	51.43 ± 10.48	58.00 ± 8.51	<0.001***
Menopause Status (%)					
Postmenopausal	142 (90.4%)	90 (93.8%)	8 (72.7%)	11 (84.6%)	0.052
Premenopausal	15 (9.6%)	6 (6.2%)	3 (27.3%)	2 (15.4%)	
FIGO Stage (%)					
Stage 1	13 (6.3%)	8 (6.4 %)	1 (7.1%)	2 (11.8%)	0.042*
Stage 2	20 (9.6%)	8 (6.4 %)	4 (28.6%)	2 (11.8%)	
Stage 3	153 (73.6%)	96 (76.8%)	9 (64.3%)	9 (52.9%)	
Stage 4	22 (10.6%)	13 (10.4%)	0 (0.0%)	4 (23.5%)	
CA 125 (mean ± SD)	1128.5 ± 1768.7	1246.4 ± 2019.7	1576.4 ± 1924.7	1053.3 ± 848.2	0.752
Residual Disease (%)					
Optimal	86 (44.1%)	51 (44.0%)	7 (53.8%)	8 (50.0%)	0.739
Suboptimal	109 (55.9%)	65 (56.0%)	6 (46.2%)	8 (50.0%)	
Histopathology (%)					
HGS	174 (81.7%)	104 (97.2%)	13 (92.9%)	16 (100.0%)	0.651
LGS	5 (2.3%)	3 (2.4%)	0 (0%)	0 (0%)	
Endometrioid	1 (0.5%)	0 (0%)	0 (0%)	0 (0%)	
OVS (months) (mean ± SD)	57.18 ± 41.32	54.11 ± 42.76	59.79 ± 35.86	76.00 ± 44.46	0.135
DFS (months) (mean ± SD)	33.32 ± 38.80	30.98 ± 40.15	26.71 ± 21.98	57.82 ± 51.31	0.031*

Statistical tests were selected based on the type of variable: the Kruskal-Wallis test was used for continuous variables such as DFS and OS, while one-way ANOVA was applied to other continuous variables (e.g., CA125 levels, age).

For categorical variables (e.g., FIGO stage, histopathology, menopausal status), Fisher's exact test was used. A significance level of $p < 0.05$ was applied throughout.

slides were scanned with 20 x 0.7NA objective with a resolution of 0.3225um (VS110, Olympus, Center Valley, PA). The mean fluorescence intensity (MFI) of each marker were quantified in the region of interest (ROI) epithelium (keratin positive cells) and stroma (region negative for cytokeratin staining) identified by Visiomorph™ (Visiopharm, Denmark). The core region included both the epithelial and stroma compartments of the tumor tissue. The CD8+ T cells density score was determined by counting CD8 positive cells per 100.000 pixels of the ROI. To validate the specificity of the antibodies used in our study, we omitted the tissue marker-specific antibodies (Figure 1; Supplementary Figure S1).

Quantitation of tissue markers

We utilized Visiomorph™ (Visiopharm, Denmark), a specialized software application designed for the analysis of digital pathology images and the identification of regions of interest (ROIs) within the tissue samples, specifically the epithelium (keratin-positive cells) and stroma (regions negative for cytokeratin staining). The mean fluorescence intensity (MFI) of each marker is then quantified within these ROIs. In the case of CD8+ T cells, we counted the

number of CD8-positive cells within each tumor tissue ROI and established a CD8+ T cell density score. This score corresponds to the number of CD8-positive cells per 100,000 pixels of ROI, providing a standardized measure of immune cell infiltration. To ensure unbiased classification and measurement, all cores were batch-processed. This approach enables the simultaneous analysis of multiple samples, minimizing the potential for human error and ensuring consistency in the quantification of markers.

Statistical analyses

Statistical analyses and data visualizations were performed using the R programming language (version 4.3.3). Associations between clinicopathologic parameters and tumor markers were analyzed using two-tailed Student's t-tests, with statistical significance set at p -value < 0.05 . To assess relationships between different tumor markers, we calculated Spearman's rank correlation coefficients, a non-parametric measure of correlation, and visualized the results using the R package "corrplot" (version 0.95). Survival analyses were performed to evaluate the prognostic significance of the markers in relation to patient outcomes,

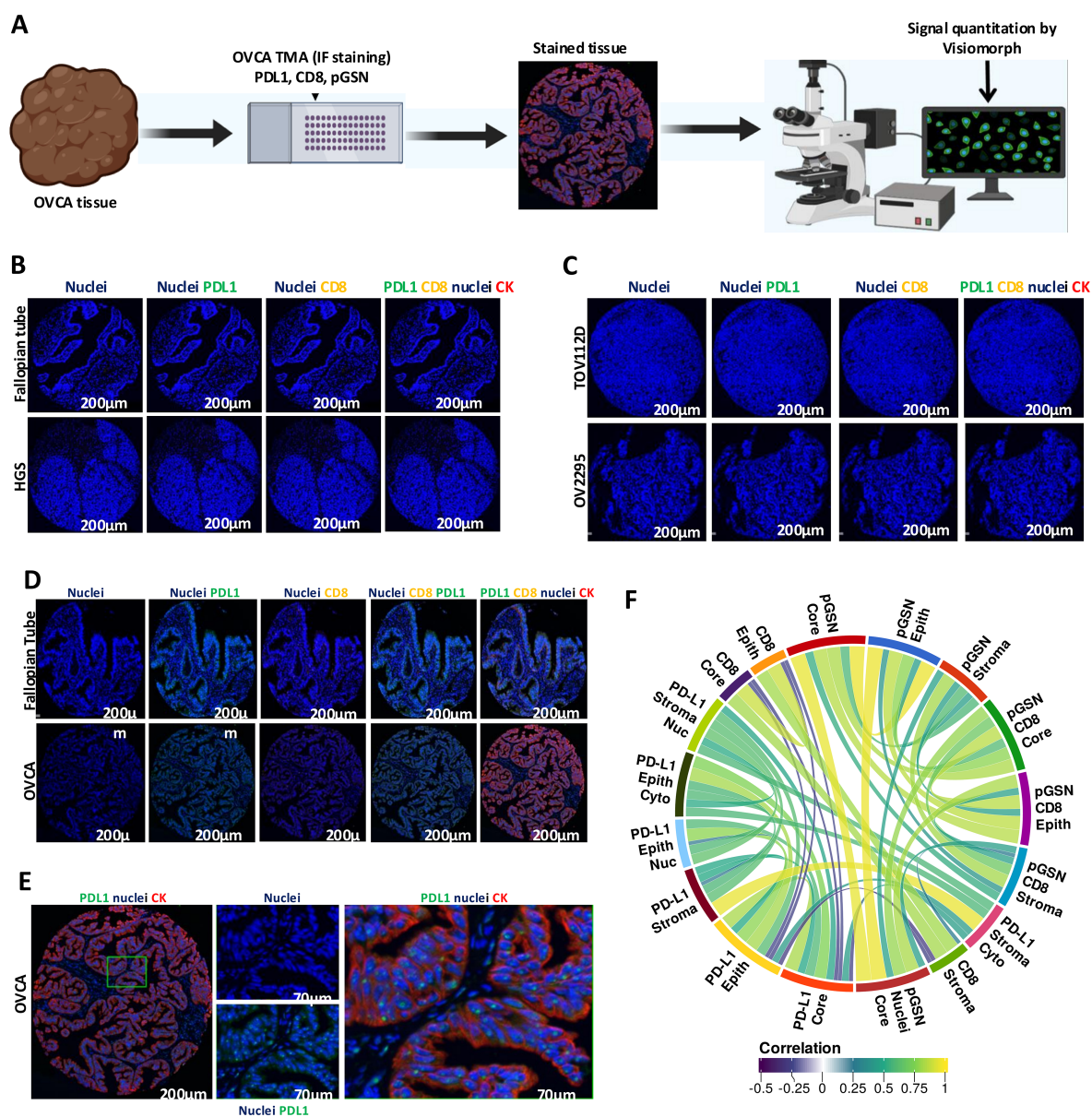


FIGURE 1 Localization of PDL1, pGSN and CD8+ T cells in ovarian cancer tissues. **(A)** Ovarian cancer tissues were immunostained with anti-cytokeratin(red), anti-PDL1 (green), and DAPI (blue) and MFI determined using Visiormorph. **(B)** Negative control validation of antibodies using normal fallopian tube and high grade serous (HGS) tissues. **(C)** Negative control validation of antibodies using cell line pellets. **(D)** immunostaining of normal fallopian tube and OVCA tissues with anti-cytokeratin(red), anti-PDL1 (green), CD8 (yellow) and DAPI (blue). **(E)** Localization of PDL1 in the nucleus of epithelial cells. **(F)** Correlative analysis of markers across tissue compartments and cellular locations. The circular visualization displays correlations between different markers (FDR < 0.01).

including overall survival (OS) and disease-free survival (DFS). For robust survival modeling and visualization, these analyses utilized the R packages “survival” (version 3.7-0) and “survminer” (version 0.5). To dichotomize marker expression values, “survminer” package was used to calculate optimal cutoff points using maximally selected rank statistics. Kaplan-Meier (KM) survival curves were generated to compare survival distributions between groups, with statistical differences assessed using the log-rank test-based p-value. Hazard ratios (HR) for clinicopathological parameters and tissue marker expression levels were determined through univariate and multivariate Cox proportional hazard

regression models. Results from these models were reported with corresponding 95% confidence intervals (CI). The multivariate survival analysis incorporated a range of clinicopathological parameters that are listed in [Table 2](#).

Machine learning based predictive modeling of chemoresistance and patient survival

We conducted a machine learning analysis to evaluate the utility of tissue marker expression levels in predicting chemoresistance.

TABLE 2 Cox proportional hazards model-based multivariable analyses of disease-free survival.

		HR		P value	
Age		0.96 (0.927 – 1.0)		0.074	
Menopause status	0	reference			
	1	2.65 (1.077 – 6.5)			0.034 *
FIGO	1	reference			
	2	16.40 (2.900 – 92.8)			0.002 **
	3	16.40 (3.143 – 85.6)			<0.001 ***
	4	36.20 (5.956 – 220.0)			<0.001 ***
CA125		0.88 (0.706 – 1.1)			0.288
RD Dichotomized	0	reference			
	1	3.15 (1.634 – 6.1)			<0.001 ***
Core PDL1		3.05 (1.589 – 5.8)			<0.001 ***
Epithelial PDL1		1.44 (0.514 – 4.0)			0.489
Stromal PDL1		1.05 (0.452 – 2.5)			0.903
Epithelial Nuclear PDL1		0.53 (0.072 – 3.9)			0.529
Epithelial Cytoplasmic PDL1		0.75 (0.135 – 4.2)			0.741
Stromal Nuclear PDL1		0.45 (0.100 – 2.0)			0.297
Stromal Cytoplasmic PDL1		2.70 (0.433 – 16.9)			0.287
Core CD8		1.55 (0.502 – 4.8)			0.447
Epithelial CD8		0.63 (0.246 – 1.6)			0.327
Stromal CD8		0.98 (0.528 – 1.8)			0.957
Core pGSN		1.48 (0.345 – 6.4)		0.597	
Epithelial pGSN		0.70 (0.214 – 2.3)		0.552	
Stromal pGSN		1.06 (0.696 – 1.6)		0.78	
Core Nuclear pGSN		1.02 (0.390 – 2.7)		0.967	
Epithelial:Cytoplasmic Ratio PDL1		0.80 (0.153 – 4.1)		0.786	
Stromal:Cytoplasmic Ratio PDL1		0.31 (0.057 – 1.6)		0.167	
BRCA1/2 Status	Wild-type	reference			
	Mutant	0.90 (0.465 – 1.8)		0.762	

Chemoresistance was defined as a progression-free interval (PFI) of ≤ 12 months, while chemosensitivity was defined as a PFI of > 12 months. Additionally, we assessed treatment responsiveness using a 6-month threshold. To build a machine learning model for chemoresistance prediction, we applied the Elastic Net algorithm, utilizing tissue marker expression values alongside clinicopathological parameters as features. We implemented a four-fold cross-validation strategy to assess model performance. In each cross-validation round, the data were spitted into a training set (75% of the data) and a validation set (25% of the data). To address class imbalance during model training, oversampling of the minority class was performed to create a more balanced

representation of both classes in the dataset. The Elastic Net parameters, alpha and lambda, were optimized using a grid search approach on the training dataset. To comprehensively assess model performance, multiple evaluation metrics were employed, including sensitivity, specificity, F1-score, and area under the curve (AUC). After optimization, we predicted outcomes for the validation data. This process was repeated four times. Posterior class probabilities from each validation set were concatenated, and the results were visualized using receiver operating characteristic (ROC) plots. Area under the curve (AUC) values were computed to quantify model performance. This analysis was performed using the R package “caret” (version 6.0-94). We trained and validated a separate

machine learning model for predicting disease-free survival (DFS). For this purpose, we used a regularized Cox regression algorithm implemented in the R package “glmnet” (version 4.1-8). Cross-validation strategy was applied as described earlier for model training and testing. Results were visualized using the R package “survivalROC” (version 1.0.3.1).

Results

Patients' characteristics

Board certified gynecologic pathologists performed the tumor staging and pathology for the 208 OVCA tissues used in the study. Details of the patients' characteristics according to their *BRCA* status are described in [Table 1](#). The median age for *BRCA* non-carriers, *BRCA1* carriers and *BRCA2* carriers are 63.14, 51.43 and 58 years, respectively. Patients enrolled in the study received no radiotherapy nor neoadjuvant chemotherapy prior to sample collection at surgery with eighty-six (86) of the patients achieving optimal cytoreduction. Optimal cytoreduction was defined as residual tumor nodules measuring ≤ 1 cm in maximum diameter, whereas suboptimal cytoreduction was defined as the presence of residual tumor nodules > 1 cm following surgery.

Tissue localization of PD-L1, pGSN and CD8+ T cells in normal fallopian tube, OVCA tissues and cell lines

Anti-PD-L1 immunotherapy has shown modest response in OVCA patients despite significant treatment responses in other solid cancers (15, 20–22, 29). The reason behind this is not fully understood. Here, we investigated how PD-L1 correlates with pGSN, a pro-survival protein, to suppress the immune system. PD-L1, pGSN and infiltrated CD8+ T cells were immunostained on a tissue microarray constructed with 208 OVCA tissues ([Table 1](#) and [Figure 1A](#)). The staining specificity of the tissue marker antibodies are shown in [Supplementary Figures 1A–H](#)). The staining of the tissue markers was optimized using normal fallopian tube, OVCA tissues and OVCA cell line-derived pellets ([Figures 1B–E](#)). The mean fluorescence intensity (MFI) was determined using the digital image analysis tool, Visiomorph. We observed no false staining or auto fluorescence in the normal and malignant tissues when no tissue marker antibody was used ([Figures 1B, C](#)). Although pGSN expression was scarcely observed in the epithelial and stromal compartments of the normal fallopian tube tissue, CD8+ T cells and PD-L1 were minimally detected ([Figure 1D](#)). Meanwhile, pGSN and PD-L1 were significantly detectable in OVCA tissues with PD-L1 localization observed in the nuclei of the epithelial compartment ([Figures 1D, E](#)). For each tissue marker expression, there was a positive correlation between compartments whereas a negative correlation was observed between PD-L1 and CD8+ T cells regardless of the tissue compartment and cellular location ([Figure 1F](#); [Supplementary Figure S1](#)).

Increased nuclear PD-L1 and pGSN expression in the epithelial and stromal compartments is associated with reduced survival impact of infiltrated CD8+ T cells

To determine the prognostic impact of nuclear PD-L1, pGSN and CD8+ T cells, MFI of their localization was detected in both the epithelial and stroma compartments. Using an MFI cut-off for each tissue marker, patients were dichotomized into high and low groups. Kaplan-Meier survival curves and log-rank tests were used to compare the survival distributions between the groups. Our results show that OVCA patients with increased nuclear PD-L1 regardless of the tissue compartment had shortened DFS and OS compared with those with decreased nuclear PD-L1 ([Figure 2](#); [Supplementary Figures S2, S3](#)). Interestingly, we observed a significant association between increased nuclear PD-L1 and poor patient survival within the epithelial (p-value= 7.3×10^{-6}) and stromal (p-value= 6.07×10^{-5}) compartments ([Figure 2](#); [Supplementary Figures S2, S3](#)). While increased infiltration of CD8+ T cells were associated with improved patient survival, patients with increased pGSN expression had shortened survival compared with others with decreased pGSN expression ([Figure 2](#); [Supplementary Figure S4–S6](#)).

We further determined if the interaction of these markers in the core, epithelial and stromal compartments affect the survival of patients. Two markers were combined at a time and patients were categorized into four (4) groups based on low and high expressions of the markers ([Figure 3](#); [Supplementary Figures S7–S9](#)). When nuclear PD-L1 and CD8 were combined in the analyses, patients with low nuclear PD-L1 and high CD8 had the most survival benefits ([Figure 3A](#), log-rank test p-value=0.001, 0.004 and 0.009 for core, epithelial and stromal, respectively). Similar results were observed within the epithelial compartment ([Figure 3B](#), log-rank test p-value=0.002, 0.003 and 0.002 for core, epithelial and stromal, respectively). The survival benefit of CD8+ T cells was however, suppressed when nuclear PD-L1 is increased, suggesting that elevated nuclear PD-L1 may suppress the survival impact of infiltrated CD8+ T cells ([Figures 3A, B](#)). A similar observation was made with overall survival when the analyses were performed using nuclear PD-L1 in the epithelial and stromal compartments ([Supplementary Figure S9](#)). When analyzing nuclear PD-L1 and pGSN together, patients with low nuclear PD-L1 and low pGSN showed the highest survival improvement, while those with high nuclear PD-L1 and high pGSN had the poorest survival outcomes ([Figure 3C](#) log-rank test p-value=0.004, 0.02 and 0.18 for core, epithelial and stromal, respectively). This effect was significant in the epithelial compartment but not the stroma ([Supplementary Figure S7](#)). A similar trend was observed when the analyses was stratified by nuclear PD-L1 in the epithelial and stromal compartments ([Supplementary Figures S8, S9](#)), suggesting that co-expression of pGSN and nuclear PD-L1 is associated with poor prognosis. We have previously demonstrated that pGSN uptake by T cells induces apoptosis, contributing to immunosuppression and chemoresistance. We confirmed this

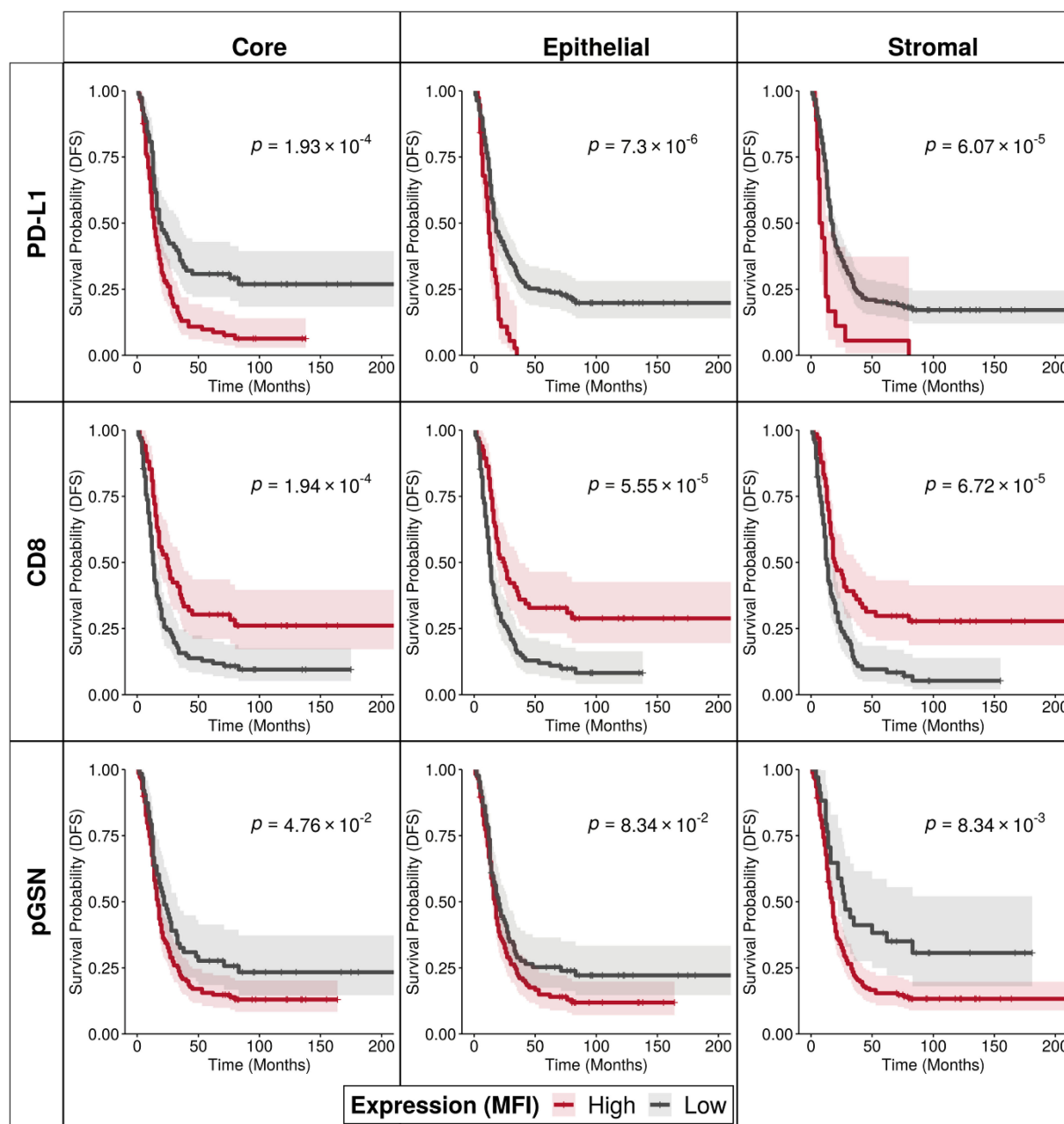


FIGURE 2

Increased nuclear PD-L1 and pGSN expressions are associated with poor patient outcome. Kaplan–Meier survival curves depicting disease-free survival for high and low expression levels of PD-L1, CD8, and pGSN proteins (indicated by rows) within the core, epithelial, and stromal compartments (indicated by columns). Expression values for each protein were dichotomized, and survival distributions between groups were compared using the log-rank test.

phenomenon as we observed increased uptake of pGSN in CD8+ T cells in patients with poor survival (Supplementary Figure S10).

BRCA1 mutations are associated with increased nuclear PD-L1 expression

Given the clinical importance of BRCA status in determining the risk for OVCA, we stratified patients based on their BRCA status and compared their tissue PD-L1, pGSN and CD8+ T cell levels.

Our results show that the carriers of BRCA1 mutation had increased levels of epithelial cytoplasmic and epithelial nuclear PD-L1 compared with non-carriers (Figures 4A, B). All other comparisons were not significant (Supplementary Figures S11–S13). We also found that the BRCA2 mutation carriers had decreased levels of epithelial and stromal pGSN compared with non-carriers (Figures 4C–F). All other BRCA2 comparisons were not significant (Supplementary Figures S14–S16). These findings reveal BRCA mutation-specific association with both PD-L1 and pGSN expressions.

Increased PD-L1 nuclear localization is associated with chemoresistance

We next assessed the association between PD-L1 nuclear localization and responsiveness to chemotherapy in patient. Chemoresistance was defined as progression free interval (PFI) \leq 12 months and chemosensitivity as PFI $>$ 12 months. We also stratified treatment responsiveness using 6 months as the criteria. Chemoresistant patients (PFI \leq 12 months) had increased levels of PD-L1 compared with chemosensitive patients (PFI $>$ 12 months) in both the epithelial and stromal compartments of the tissue (Figures 4G–I; Supplementary Figures S17–S21). There was no significant difference observed with nuclear and cytoplasmic PD-L1 when the 6 months criteria were used (Supplementary Figures S19–S21). On the contrary, chemosensitive patients had increased

infiltration of CD8⁺ T cells in the epithelial and stromal compartments (Figures 4J–L). This difference was regardless of the criteria used for defining treatment response (6- and 12-months, Supplementary Figure S20). When using 6-months PFI criteria, we observed significant association with chemosensitivity for stromal pGSN, and pGSN colocalized in CD8 T cells in the epithelial and stromal compartments (Supplementary Figure S21).

We next examined the combined effect of PD-L1 and CD8⁺ T cells on chemoresistance (Figure 5A). In the high PD-L1 and low CD8 group, 52% of patients were chemoresistant, whereas only 21% of patients in the low PD-L1 and high CD8 group were chemoresistant. These findings highlight the poor prognostic characteristic of PD-L1 expression in OVCA patients as well as suggest an inverse relationship between PD-L1 expression and CD8⁺ T cell levels in predicting chemoresistance.

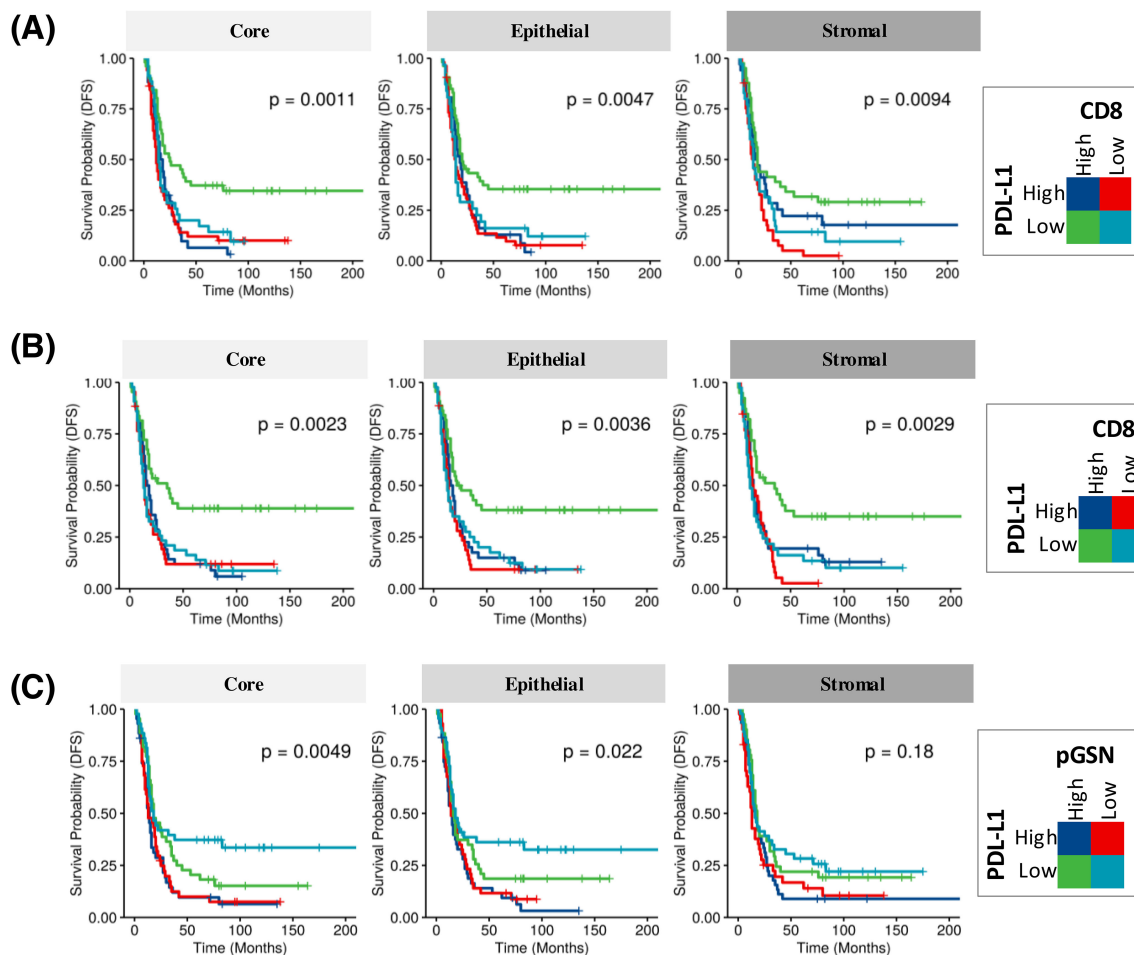
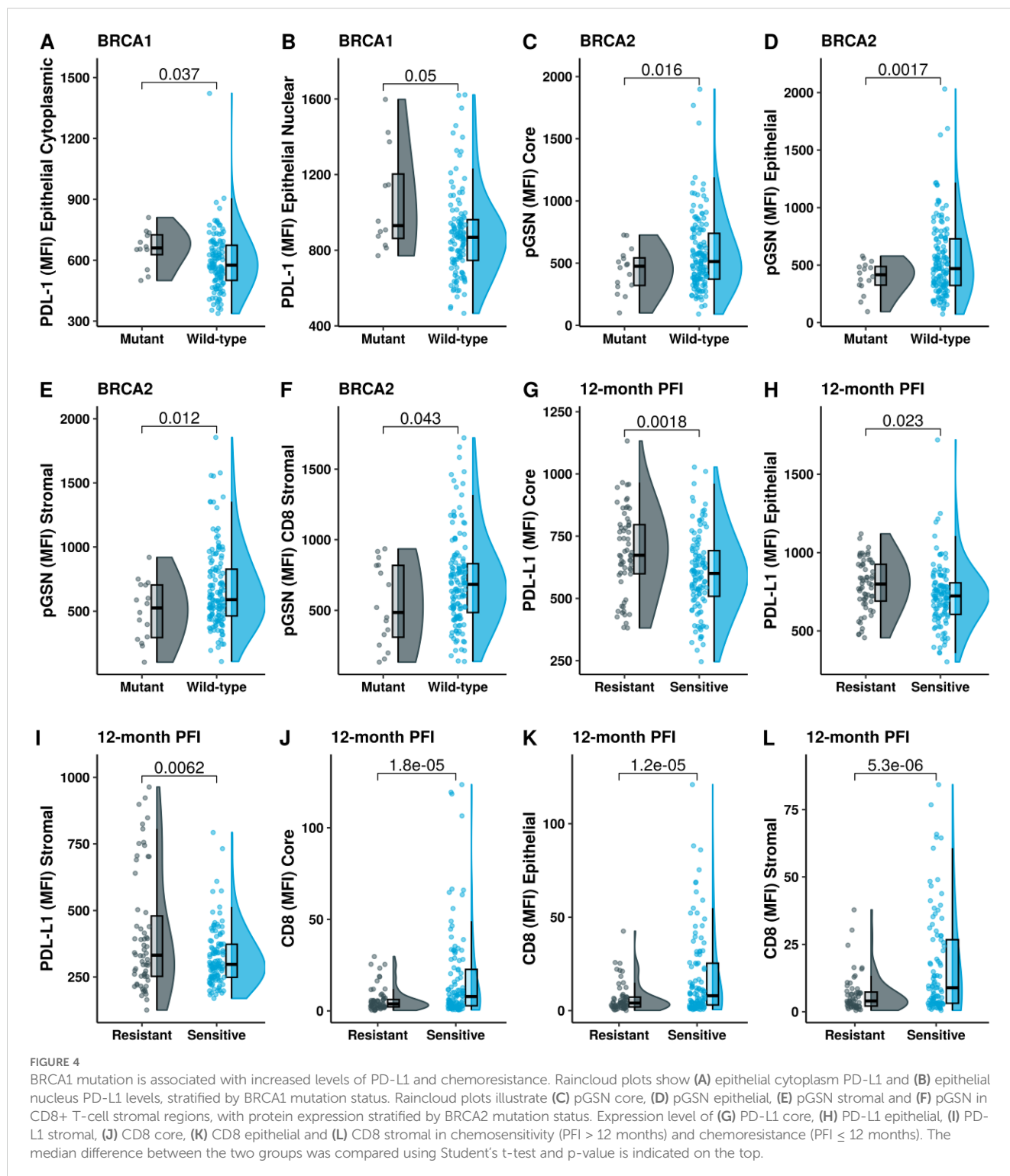


FIGURE 3

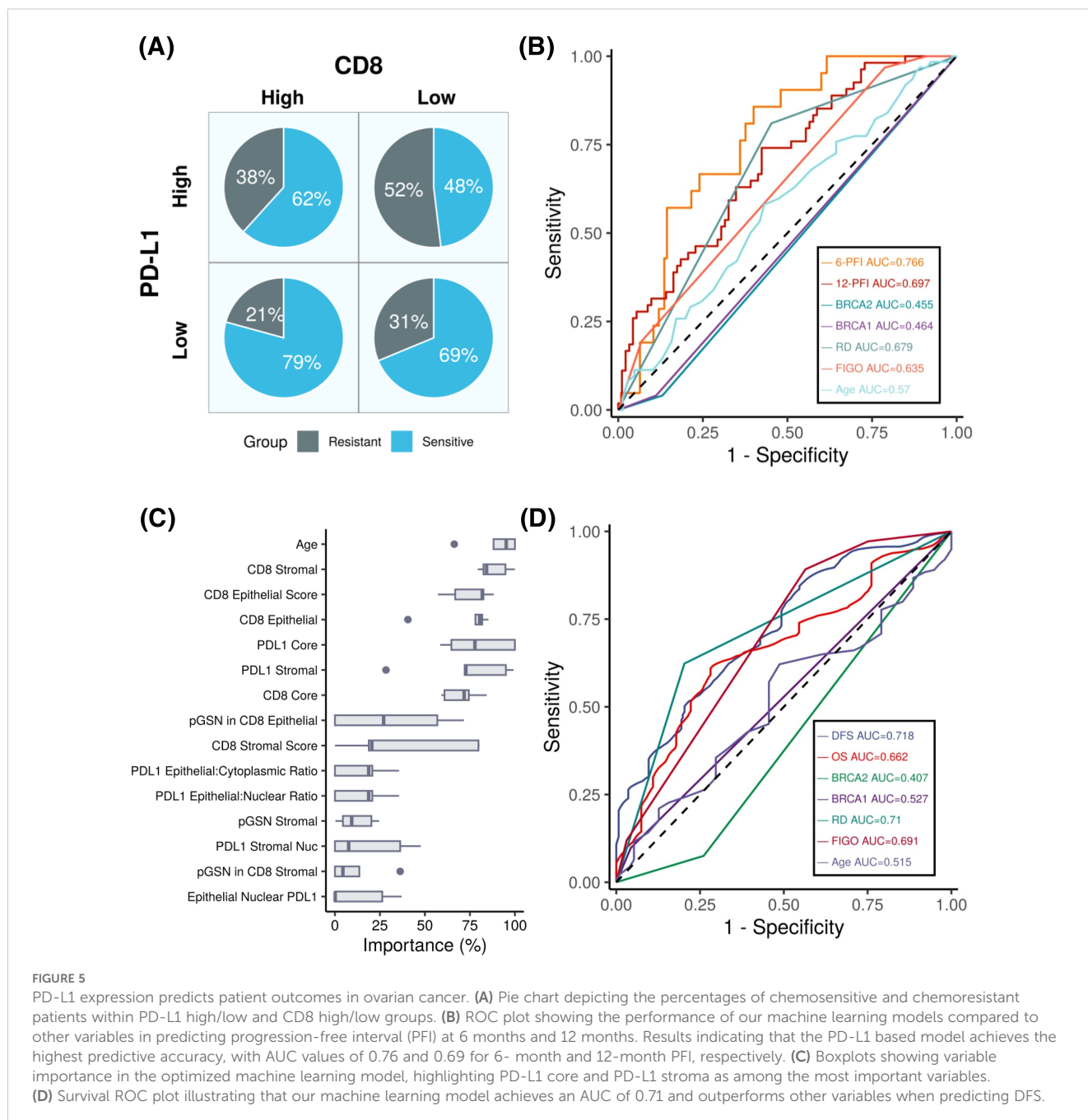
Increased nuclear PD-L1 and pGSN hinder the anti-tumor benefits of infiltrated CD8⁺ T cells in the OVCA microenvironment and associated with disease-free survival (DFS). KM plot in (A) shows PD-L1 expression in combination with infiltrated CD8⁺ T cells in the core, epithelial and stromal compartments. (B) Epithelial nuclear PD-L1 expression in combination with CD8⁺ T cell presence in the core, epithelium, and stroma. (C) PD-L1 expression in combination with pGSN expression in the core, epithelium, and stroma. For the analysis, samples were classified into four groups based on the expression levels of two markers. Each marker was dichotomized into high and low expression, resulting in four groups: high-high, high-low, low-high, and low-low. Kaplan–Meier survival plots depict disease-free survival probabilities across these groups for the respective markers. Survival distributions were compared using the log-rank test.



Prognostic impact of PD-L1, pGSN, CD8+ T cells

To determine the prognostic impact of the tissue markers together with clinicopathological parameters in predicting DFS and OS, we used univariate and multivariate Cox regression analyses (Table 2; Supplementary Tables S1–S3). From the univariate Cox regression analysis, we observed that age, FIGO

stages 3 and 4, residual disease, PD-L1 (core, epithelial and stroma), nuclear PD-L1 (epithelial and stroma), cytoplasm PD-L1 (epithelial and stroma), CD8 (core, epithelial and stroma), pGSN core, epithelial pGSN and nuclear pGSN were significantly associated with OS (Supplementary Table S1). For DFS, FIGO stages 3 and 4, residual disease, PD-L1 (core, epithelial and stroma), nuclear PD-L1 (epithelial and stroma), cytoplasm PD-L1 (epithelial and stroma), CD8 (core, epithelial and stroma) and *BRCA2* status significantly



predicted DFS (Supplementary Table S2). In the multivariate Cox regression analysis, menopausal status, FIGO stage, residual disease, and PD-L1 core were significant predictors of disease-free survival (Table 2). These findings were consistent when the analysis performed for overall survival (Supplementary Table S3). Next, we evaluated the chemosensitivity prediction and prognostic potential of the selected markers. Using marker expression values and clinical data, we developed an Elastic Net-based machine learning model to predict chemoresistance (PFI \leq 12 months) and chemosensitivity (PFI $>$ 12 months). Cross-validation demonstrated that the model achieved an area under the curve (AUC) value of 0.697 (Figure 5B). Notably, when predicting PFI at 6 months, the model's performance improved, yielding an AUC value

of 0.766. This model outperformed other clinical variables in predicting chemoresistance. To identify the most influential variables in the machine learning model, we conducted a variable importance analysis (Figure 5C). The results indicated that PD-L1 core, PD-L1 stroma and different CD8 markers were among the most critical features selected by the model. Additionally, we trained a separate Elastic Net-based model to predict disease-free survival (DFS) using protein marker expression and clinical data (Figure 5D). Cross-validation showed that the model achieved an AUC of 0.718 for DFS prediction and 0.662 for OS prediction. Comparisons with AUC values derived from clinical variables alone confirmed that DFS prediction demonstrated superior performance. In summary, our findings highlight that the

markers such as PD-L1, pGSN, and CD8+ T cells are robust predictors of chemoresistance and can reliably predict patient survival outcomes.

Discussion

Anti-PD-L1 immunotherapy has achieved only a modest therapeutic success in OVCA patients despite significant therapeutic success in other solid tumors (21, 22). Although there are extensive studies on cyto-membranal PD-L1, scarce attention has been given to the nuclear localization of PD-L1 and its clinical significance in OVCA and other cancer type (26, 28). In this study, our findings highlight the prognostic value of nuclear PD-L1 and its relationship with pGSN and CD8+ T cells. Furthermore, our study provides a potential explanation for the modest therapeutic response observed with anti-PD-L1 therapies.

Increased PD-L1 expression in the epithelial and stromal compartments of the tissues was associated with shortened OS and DFS. In this context our findings are consistent with previous studies that have reported similar findings in other cancers (18, 30, 31). When stratified by cellular location, we observed the most significant effect with nuclear PD-L1, suggesting a potential prognostic value. Although increased infiltration of CD8+ T cells provided survival benefits to patients, these survival benefits were significantly hindered by nuclear PD-L1 elevation, a phenomenon that we had previously seen with pGSN also (9). Interestingly, patients with elevated pGSN and nuclear PD-L1 had the worst survival, suggesting a synergistic pro-tumor effect of both markers. Chemoresistance presents as a major obstacle in achieving therapeutic success in OVCA patients. Our previous studies have shown a significant association between elevated pGSN and chemoresistance (8, 10, 12). In addition to confirming this phenomenon in our current study, we have also demonstrated a significant association between epithelial expression of PD-L1 and chemoresistance.

Anti-PD-L1 antibodies bind and inhibit PD-L1 on the surface of cancer cells, thus, preventing its interaction with PD-1 (32). The authors observed that the inhibition was associated with increased presence of nuclear PD-L1, thus, rendering the therapeutic effects of anti-PD-L1 ineffective. Nuclear PD-L1 has been detected as a poor prognostic marker in breast cancer, lung adenocarcinoma, renal cell carcinoma, hepatocellular carcinoma, and prostate cancer (24–28). In uveal melanoma, nuclear PD-L1 promotes early growth response-1 (EGR1)-mediated angiogenesis and tumorigenesis (28). Yang Gao, et al., have shown that PD-L1 translocate into the nucleus via an acetylation-dependent pathway and blocking its translocation resulted in an enhanced therapeutic efficacy of PD-1/PD-L1 inhibitor treatment (24). pGSN induces HIF1alpha-mediated chemoresistance in OVCA cells while HIF1alpha drives PD-L1 transcription leading to poor anti-PD-L1 response (8, 26, 33). We therefore hypothesize that pGSN activates HIF1alpha-mediated PD-L1 transcription resulting in the expression of tumor promoting and immune-suppressive genes, a process

leading to tumor recurrence, chemoresistance and poor overall survival.

We also compared the relative levels of PD-L1, pGSN and CD8+ T cells between carriers and non-carriers of *BRCA1/2* mutations as well as how these mutations relate to chemoresistance and patient survival. We found that PD-L1 was elevated in *BRCA1* mutation carriers while pGSN was downregulated in *BRCA2* mutation carriers. *BRCA1/2* characterization may therefore provide clinicians with prior information about pGSN and PD-L1 expression in the OVCA microenvironment in personalized therapeutic options.

The current study despite its key findings, has a few limitations. The tissues were retrospectively collected with no prospective collections. The Canadian Ovarian Experimental Unified Resource (COEUR) manages the collection of tissues and adheres to the standards defined by the Canadian Tissue Repository Network (CTRNet), which ensures the quality of the biological material (34). Thus, we don't anticipate any interferences with our staining. Although we attempted to mitigate biases associated with treatment heterogeneity by controlling for critical factors, such as genetic mutations and relevant clinical parameters in statistical analysis, treatment variability may still have influenced survival outcomes- a common limitation in cohort-based studies. However, our methodology, analyzing both PFS and OS, along with rigorous adjustment for treatment-related factors has helped to substantially reduce the potential impact of these biases. We did not perform functional experiments, which restricts our ability to confirm the mechanistic relevance of the observed associations. Lastly, pGSN staining was conducted on a separate tissue panel, preventing us from providing a co-localization image with PD-L1 or CD8+ T cells within the same tumor microenvironment. Future studies will investigate the *in vitro* and *in vivo* mechanistic interaction between nuclear PD-L1 and pGSN and how that promotes chemoresistance in OVCA.

For the first time, we have provided convincing evidence about the detection and prognostic value of nuclear PD-L1 in OVCA. We have shown that elevated PD-L1 together with pGSN suppress the anti-tumor functions of CD8+ T cell contributing to OVCA recurrence, chemoresistance and poor overall survival.

Data availability statement

The original contributions presented in the study are included in the article/[Supplementary Material](#). Further inquiries can be directed to the corresponding authors.

Ethics statement

The studies involving humans were approved by the Centre hospitalier de l'Université de Montreal (CHUM) Ethics Committee [Montreal, Quebec, Canada, Institutional Review Board (IRB) approval number, BD 04-002] and the Ottawa Health Science

Network Research Ethics Board (Ottawa, Ontario, Canada, IRB approval number, OHSN-REB 1999540-01H). The studies were conducted in accordance with the local legislation and institutional requirements. The human samples used in this study were acquired from primarily isolated as part of your previous study for which ethical approval was obtained. Written informed consent for participation was not required from the participants or the participants' legal guardians/next of kin in accordance with the national legislation and institutional requirements.

Author contributions

MA-W: Writing – original draft, Writing – review & editing. AZ: Writing – original draft, Writing – review & editing. ST: Writing – original draft. LC: Writing – review & editing, Writing – original draft. EC: Writing – review & editing, Writing – original draft. AM-M: Writing – review & editing, Writing – original draft. BT: Writing – original draft, Writing – review & editing. AM: Writing – original draft, Writing – review & editing.

Funding

The author(s) declare that financial support was received for the research and/or publication of this article. This work was supported in part by the Canadian Institutes of Health Research (PJT-168949; awarded to Dr. Benjamin K. Tsang), Mitacs Globalink Research Award, Ovarian Cancer Canada (OCC) and Taggart-Parkes Fellowship (awarded to Dr. Meshach Asare-Werehene). Tumor banking was supported by the Banque de tissus et de données of the Réseau de recherche sur le cancer du Fonds de recherche du

Québec – Santé (FRQS), associated with the Canadian Tissue Repository Network. A.-M. Mes-Masson is a researcher of the CRHUM which receives support from the FRQS.

Conflict of interest

The authors declare that the research was conducted in the absence of any commercial or financial relationships that could be construed as a potential conflict of interest.

Generative AI statement

The author(s) declare that no Generative AI was used in the creation of this manuscript.

Publisher's note

All claims expressed in this article are solely those of the authors and do not necessarily represent those of their affiliated organizations, or those of the publisher, the editors and the reviewers. Any product that may be evaluated in this article, or claim that may be made by its manufacturer, is not guaranteed or endorsed by the publisher.

Supplementary material

The Supplementary Material for this article can be found online at: <https://www.frontiersin.org/articles/10.3389/fimmu.2025.1543529/full#supplementary-material>

References

- Brenner DR, Gillis J, Demers AA, Ellison LF, Billette JM, Zhang SX, et al. Projected estimates of cancer in Canada in 2024. *CMAJ*. (2024) 196(18):E615–23.
- Bray F, Ferlay J, Soerjomataram I, Siegel RL, Torre LA, Jemal A. Global cancer statistics 2018: GLOBOCAN estimates of incidence and mortality worldwide for 36 cancers in 185 countries. *CA Cancer J Clin*. (2018) 68:394–424. doi: 10.3322/caac.21492
- Doo DW, Norian LA, Arend RC. Checkpoint inhibitors in ovarian cancer: A review of preclinical data. *Gynecol Oncol Rep*. (2019) 29:48–54. doi: 10.1016/j.gore.2019.06.003
- Ghisoni E, Imbimbo M, Zimmermann S, Valabrega G. Ovarian cancer immunotherapy: turning up the heat. *Int J Mol Sci*. (2019) 20(12):2927. doi: 10.3390/ijms20122927
- Hao D, Liu J, Chen M, Li J, Wang L, Li X, et al. Immunogenomic analyses of advanced serous ovarian cancer reveal immune score is a strong prognostic factor and an indicator of chemosensitivity. *Clin Cancer Res*. (2018) 24:3560–71. doi: 10.1158/1078-0432.CCR-17-3862
- McCloskey CW, Rodriguez GM, Galpin KJC, Vanderhyden BC. Ovarian cancer immunotherapy: preclinical models and emerging therapeutics. *Cancers (Basel)*. (2018) 10(8):244. doi: 10.3390/cancers10080244
- Pogge von Strandmann E, Reinartz S, Wager U, Müller R. Tumor-host cell interactions in ovarian cancer: pathways to therapy failure. *Trends Cancer*. (2017) 3:137–48. doi: 10.1016/j.trecan.2016.12.005
- Asare-Werehene M, Nakka K, Reunov A, Chiu CT, Lee WT, Abedini MR, et al. The exosome-mediated autocrine and paracrine actions of plasma gelsolin in ovarian cancer chemoresistance. *Oncogene*. (2020) 39:1600–16. doi: 10.1038/s41388-019-1087-9
- Asare-Werehene M, Communal L, Carmona E, Han Y, Song YS, Burger D, et al. Plasma gelsolin inhibits CD8(+) T-cell function and regulates glutathione production to confer chemoresistance in ovarian cancer. *Cancer Res*. (2020) 80:3959–71. doi: 10.1158/0008-5472.CAN-20-0788
- Asare-Werehene M, Tsuyoshi H, Zhang H, Salehi R, Chang CY, Carmona E, et al. Plasma gelsolin confers chemoresistance in ovarian cancer by resetting the relative abundance and function of macrophage subtypes. *Cancers (Basel)*. (2022) 14(4):1039. doi: 10.3390/cancers14041039
- Giampazolias E, Schulz O, Lim KHJ, Rogers NC, Chakravarty P, Srinivasan N, et al. Secreted gelsolin inhibits DNGR-1-dependent cross-presentation and cancer immunity. *Cell*. (2021) 184:4016–31.e22. doi: 10.1016/j.cell.2021.05.021
- Onuma T, Asare-Werehene M, Fujita Y, Yoshida Y, Tsang BK. Plasma gelsolin inhibits natural killer cell function and confers chemoresistance in epithelial ovarian cancer. *Cells*. (2024) 13(11):905. doi: 10.3390/cells13110905
- Pardoll DM. The blockade of immune checkpoints in cancer immunotherapy. *Nat Rev Cancer*. (2012) 12:252–64. doi: 10.1038/nrc3239
- Kornepati AVR, Vadlamudi RK, Curiel TJ. Programmed death ligand 1 signals in cancer cells. *Nat Rev Cancer*. (2022) 22:174–89. doi: 10.1038/s41568-021-00431-4
- Wan C, Keany MP, Dong H, Al-Alem LF, Pandya UM, Lazo S, et al. Enhanced efficacy of simultaneous PD-1 and PD-L1 immune checkpoint blockade in high-grade serous ovarian cancer. *Cancer Res*. (2021) 81:158–73. doi: 10.1158/0008-5472.CAN-20-1674
- Høgdaal E, Høgdaal C, Vo T, Zhou W, Huang L, Marton M, et al. Impact of PD-L1 and T-cell inflamed gene expression profile on survival in advanced ovarian cancer. *Int J Gynecol Cancer*. (2020) 30:1034–42. doi: 10.1136/ijgc-2019-001109

17. Alwosaibai K, Aalmri S, Mashhour M, Ghandorah S, Alshangiti A, Azam F, et al. PD-L1 is highly expressed in ovarian cancer and associated with cancer stem cells populations expressing CD44 and other stem cell markers. *BMC Cancer*. (2023) 23:13. doi: 10.1186/s12885-022-10404-x
18. Hamanishi J, Mandai M, Iwasaki M, Okazaki T, Tanaka Y, Yamaguchi K, et al. Programmed cell death 1 ligand 1 and tumor-infiltrating CD8+ T lymphocytes are prognostic factors of human ovarian cancer. *Proc Natl Acad Sci U S A*. (2007) 104:3360–5. doi: 10.1073/pnas.0611533104
19. Webb JR, Milne K, Kroeger DR, Nelson BH. PD-L1 expression is associated with tumor-infiltrating T cells and favorable prognosis in high-grade serous ovarian cancer. *Gynecol Oncol*. (2016) 141:293–302. doi: 10.1016/j.ygyno.2016.03.008
20. Peng Z, Li M, Li H, Gao Q. PD-1/PD-L1 immune checkpoint blockade in ovarian cancer: Dilemmas and opportunities. *Drug Discov Today*. (2023) 28:103666. doi: 10.1016/j.drudis.2023.103666
21. Zhu J, Yan L, Wang Q. Efficacy of PD-1/PD-L1 inhibitors in ovarian cancer: a single-arm meta-analysis. *J Ovarian Res*. (2021) 14:112. doi: 10.1186/s13048-021-00862-5
22. Chardin L, Leary A. Immunotherapy in ovarian cancer: thinking beyond PD-1/PD-L1. *Front Oncol*. (2021) 11:795547. doi: 10.3389/fonc.2021.795547
23. Javed SA, Najmi A, Ahsan W, Zoghebi K. Targeting PD-1/PD-L1 immune checkpoint inhibition for cancer immunotherapy: success and challenges. *Front Immunol*. (2024) 15:1383456. doi: 10.3389/fimmu.2024.1383456
24. Gao Y, Nihira NT, Bu X, Chu C, Zhang J, Kolodziejczyk A, et al. Acetylation-dependent regulation of PD-L1 nuclear translocation dictates the efficacy of anti-PD-1 immunotherapy. *Nat Cell Biol*. (2020) 22:1064–75. doi: 10.1038/s41556-020-0562-4
25. Xiong W, Gao Y, Wei W, Zhang J. Extracellular and nuclear PD-L1 in modulating cancer immunotherapy. *Trends Cancer*. (2021) 7:837–46. doi: 10.1016/j.trecan.2021.03.003
26. Qu L, Jin J, Lou J, Qian C, Lin J, Xu A, et al. The nuclear transportation of PD-L1 and the function in tumor immunity and progression. *Cancer Immunol Immunother*. (2022) 71:2313–23. doi: 10.1007/s00262-022-03176-7
27. Lee JJ, Kim SY, Kim SH, Choi S, Lee B, Shin JS. STING mediates nuclear PD-L1 targeting-induced senescence in cancer cells. *Cell Death Dis*. (2022) 13:791. doi: 10.1038/s41419-022-05217-6
28. Yu J, Zhuang A, Gu X, Hua Y, Yang L, Ge S, et al. Nuclear PD-L1 promotes EGR1-mediated angiogenesis and accelerates tumorigenesis. *Cell Discov*. (2023) 9:33. doi: 10.1038/s41421-023-00521-7
29. Hamanishi J, Mandai M, Ikeda T, Minami M, Kawaguchi A, Murayama T, et al. Safety and antitumor activity of anti-PD-1 antibody, nivolumab, in patients with platinum-resistant ovarian cancer. *J Clin Oncol*. (2015) 33:4015–22. doi: 10.1200/JCO.2015.62.3397
30. Wang L. Prognostic effect of programmed death-ligand 1 (PD-L1) in ovarian cancer: a systematic review, meta-analysis and bioinformatics study. *J Ovarian Res*. (2019) 12:37. doi: 10.1186/s13048-019-0512-6
31. Wang JJ, Siu MK, Jiang YX, Leung TH, Chan DW, Cheng RR, et al. Aberrant upregulation of PDK1 in ovarian cancer cells impairs CD8(+) T cell function and survival through elevation of PD-L1. *Oncoimmunology*. (2019) 8:e1659092. doi: 10.1080/2162402X.2019.1659092
32. Sunshine J, Taube JM. PD-1/PD-L1 inhibitors. *Curr Opin Pharmacol*. (2015) 23:32–8. doi: 10.1016/j.coph.2015.05.011
33. Ruf M, Moch H, Schraml P. PD-L1 expression is regulated by hypoxia inducible factor in clear cell renal cell carcinoma. *Int J Cancer*. (2016) 139:396–403. doi: 10.1002/ijc.30077
34. Le Page C, Rahimi K, Köbel M, Tonin PN, Meunier L, Portelance L, et al. Characteristics and outcome of the COEUR Canadian validation cohort for ovarian cancer biomarkers. *BMC Cancer*. (2018) 18:347. doi: 10.1186/s12885-018-4242-8